

3D MODELING AND SIMULATIONS OF ELECTRON EMISSION FROM PHOTOCATHODES WITH CONTROLLED ROUGH SURFACES*

D. A. Dimitrov, G. I. Bell, D. Smithe, C. Zhou, Tech-X Corp., Boulder, CO 80303, USA
 I. Ben-Zvi, J. Smedley, BNL, Upton, NY 11973, USA
 S. Karkare, H. A. Padmore, LBNL, Berkeley, CA 94720, USA

Abstract

Developments in materials design and synthesis have resulted in photocathodes that can have a high quantum efficiency (QE), operate at visible wavelengths, and are robust enough to operate in high electric field gradient photoguns, for application to free electron lasers and in dynamic electron microscopy and diffraction. However, synthesis often results in roughness, ranging from the nano to the microscale. The effect of this roughness in a high gradient accelerator is to produce a small transverse accelerating gradient, which therefore results in emittance growth. Although analytical formulations of the effects of roughness have been developed, a full theoretical model and experimental verification are lacking, and our work aims to bridge this gap. We report results on electron emission modeling and 3D simulations from photocathodes with controlled surface roughness similar to grated surfaces that have been fabricated by nanolithography. The simulations include both charge carrier dynamics in the photocathode material and a general electron emission modeling that includes field enhancement effects at rough surfaces. The models are being implemented in the VSIm code.

INTRODUCTION

Successful operation of modern X-ray light sources, free electron laser (FEL), and linear accelerator facilities depends on providing reliable photocathodes [1] for generation of low emittance, high-brightness, high-current electron beams using conventional lasers.

Developments in materials design and synthesis have resulted in photocathodes that can have a high quantum efficiency (QE), operate at visible wavelengths, and are robust enough to operate in high electric field gradient photoguns, for application to free electron lasers and in dynamic electron microscopy and diffraction. However, synthesis often results in roughness, ranging from the nano to the microscale. Thus, the effects on roughness on emittance are of significant importance to understand.

Recent advances in material science methods have been demonstrated to control the growth of photoemissive materials (e.g. Sb) on a substrate to create different types of rough layers with a variable thickness of the order of 10 nm. An example of such photoemissive layer with controlled sinusoidal roughness is shown in Fig. 1 together with the overall diagram of momentatron experiments developed [2] to measure transverse electron momentum and emittance.

* We are grateful to the U.S. DoE Office of Basic Energy Sciences for supporting this work under the grant DE-SC0013190.

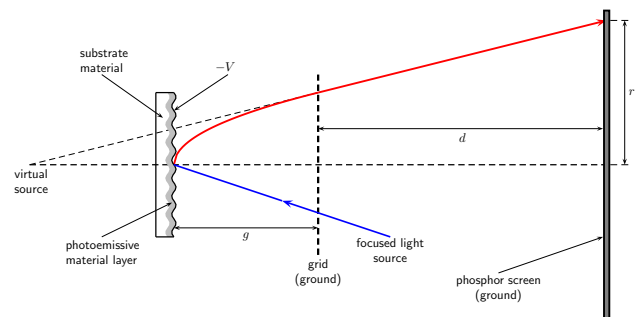


Figure 1: Diagram (not to scale) of momentatron experiments for measurement of transverse momentum of emitted electrons using rough (shown) and flat photocathode surfaces.

Feng *et al.* [3] showed recently how data from momentatron experiments can be used to investigate the thermal limit of intrinsic emittance of metal photocathodes.

Although analytical formulations of the effects of roughness have been developed, a full theoretical model and experimental verification are lacking, and our work aims to bridge this gap. We report results on electron emission modeling and 3D simulations from photocathodes with controlled surface roughness similar to grated surfaces that have been fabricated by nanolithography and investigated in momentatron experiments. The simulations include both charge carrier dynamics in the photocathode material and a general electron emission modeling with field enhancement effects at rough surfaces.

MODELING

The overall modeling capabilities needed (within the framework of a Particle-in-Cell (PIC) code) to simulate electron emission from photocathodes with controlled rough surfaces consist of: (i) electron excitation in a photoemissive material in response to absorption of photons with a given wavelength, (ii) charge dynamics due to drift and various types of scattering processes, (iii) representation of rough interfaces, (iv) calculation of electron emission probabilities that takes into account image charge and field enhancement effects across rough surfaces, (v) particle reflection and emission updates and efficient 3D electrostatic (ES) solver for a simulation domain that has sub-domains with different dielectric properties separated by piece-wise continuous rough interfaces.

Electron excitation is modeled with exponential decay of absorbed laser light intensity relative to positions on the photocathode surface. Here, we implemented and used a

model for electron excitation due to normal light incidence (to a plane tangent to the same height tips of a controlled rough surface). Electrons are selected for excitation from occupied states at a given temperature T in a metallic conduction band with a free electron density of states (DOS) and are excited only to unoccupied states (practically all with energies $E > \mu(T)$, where $\mu(T)$ is the chemical potential).

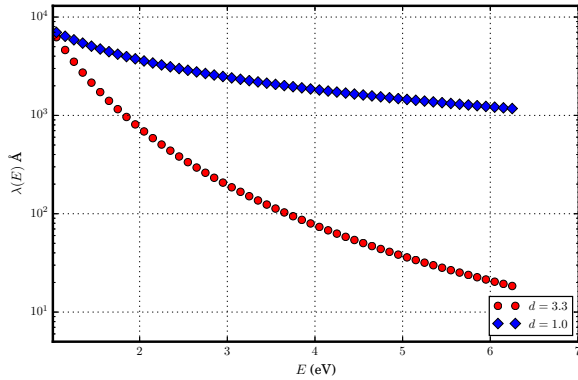


Figure 2: Electron-electron scattering mean free paths calculated using the generalized model proposed by Ziaja *et al.* [4].

In VSim, we have already implemented models for charge transport in two semiconductor materials: diamond [5] and GaAs [6]. These models take into account different types of electron and hole scattering processes.

However, metals and semi-metals have been of interest to investigate in momentum experiments. In these materials, the electron-electron scattering is the dominant process that affects emission with usually one such process reducing the energy of an excited electron below its threshold for emission. In order to model emission from such materials, we have recently implemented a model for electron-electron scattering in metals proposed by Ziaja *et al.* [4]. It is a unified model for calculation of electron-electron scattering rates in metals and semiconductors that is applicable over a wide range of energies and is efficient for use in Monte Carlo transport simulations. In their approach, the electron mean free path (MFP), $\lambda(E)$, is given by the simple formula:

$$\lambda(E) = \frac{\sqrt{E}}{a(E - E_{th})^b} + \frac{E - E_0 \exp(-B/A)}{A \ln(E/E_0) + B}, \quad (1)$$

where the electron energy E is given in eV, E_{th} is the effective energy threshold for the scattering process ($E_{th} = E_F$ for metals with E_F being the Fermi level), $E_0 = 1$ eV, and a , b , A , and B are fitting parameters with units that give the MFP in Å when evaluated via Eq. (1). The electron scattering rate $\Gamma(E)$ can be calculated in a straightforward way once $\lambda(E)$ is known. The fitting parameters are determined using experimental data and/or full band structure calculations (when available) for any material of interest. The parameters a and b determine the MFP at the low energy regime ($E < E_P$, where E_P is the plasmon energy). This is the regime of interest to electron emission from metallic materials. Then, Eq.(1) reduces to $\lambda(E) \approx c/E^d$ with electron

energies measured relative to E_F (thus $E_{th} = 0$), $c = 1/a$, and $d = b - 1/2$. In Fig. 2, we show the MFPs for two values of the d parameter that we used to model electron-electron scattering in Sb. Since we currently do not have data for this type of scattering in Sb, we bracketed the MFPs over the range shown in Fig. 2 (MFPs for different metals [4] have been reported in this range).

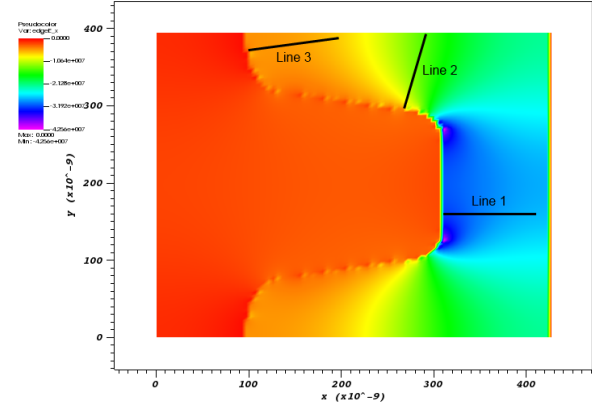


Figure 3: Longitudinal electric field from VSim's ES solver for the case of a single ridge rough surface confirms the strongest field enhancement is close to the tips of the ridge. The lines shown are normal to the ridge surface at the corresponding locations. The ES potential is calculated along such normals at positions where electrons attempt to cross the surface in order to calculate emission probabilities.

When an electron from inside the photocathode attempts to cross the emission surface, a probability of emission is calculated using our implementation of the transfer matrix (TM) method [7] with a surface potential determined at the location of the crossing and along the outward normal as shown in Fig. 3. This allows us to take into account the field enhancement effect. The surface intersection shown in Fig. 3 is for one ridge rough surface represented in VSim with a stair-step grid boundary.

RESULTS

We ran simulations with the implemented electron-electron scattering model to investigate how controlled surface roughness and two different MFP regimes affect quantum efficiency over a range of photon excitation energies. Emission was simulated from Sb (work function of 4.4 eV) with a flat and a three-ridge rough surfaces with periodic boundary conditions along the transverse directions (y and z). There is a constant potential difference maintained across the x length of the simulation domain leading to an applied field magnitude in the vacuum region of the order of 1 MV/m (it varies on the rough emission surface).

The controlled rough surface has a ridge period of 394 nm, ridge height of 194 nm, and a width of the ridge flat top of 79 nm. The three ridge rough surface is shown in Fig. 4 together with excited electrons and their distribution at a given time. The simulation domain size for both the 3-ridge and the flat emission surfaces is $0.4268 \times 1.182 \times 0.394$ all in μm along

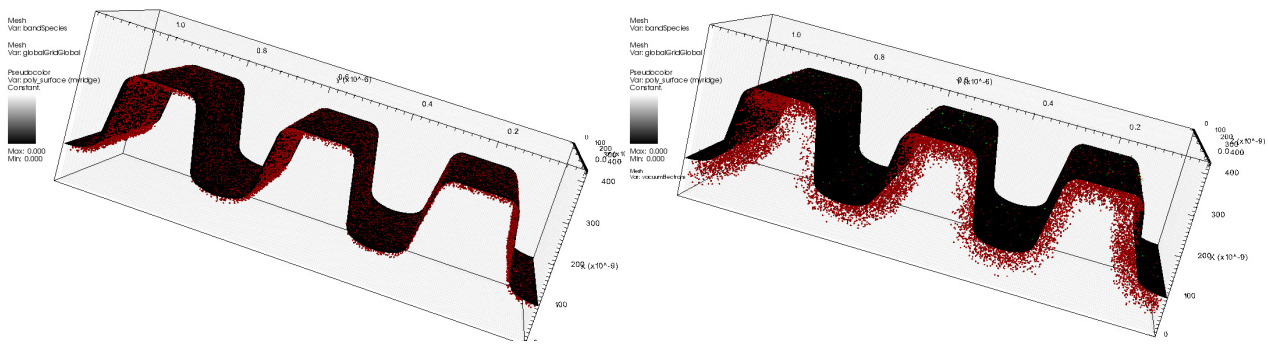


Figure 4: Electrons are loaded only at $t = 0$ s (left plot) in the Sb sub-domain of the simulation (shown with red spheres) and within a layer of 20 nm from the rough vacuum interface (shown with semi-transparent gray surface). The electron dynamics in Sb is practically diffusive with only a small number emitted into the vacuum sub-domain (shown with green spheres in the right plot at simulation time of 25 fs).

x , y , and z respectively with $88 \times 264 \times 16$ number of cells. The time step was set to 2.5×10^{-16} s and the simulations were ran for 2000 time steps. We implemented an algorithm

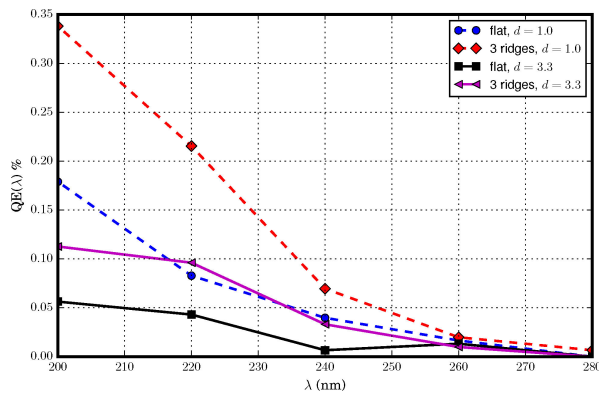


Figure 5: As expected, the QE increases when decreasing photon excitation wavelength. The results are from simulations in response to absorption of around 30000 photons at $t = 0$ s only, flat and 3-ridge emission surfaces, and two cases of electron-electron scattering rates.

that removes electrons in the photocathode if their energy falls below a given threshold value that effectively is not sufficient for emission. Due to electron-electron scattering, most of the excited electrons loaded at $t = 0$ have been removed by the end of the simulation. For the Sb parameters (and for metals), practically one electron-electron scattering event reduces the energy of an excited electron enough to make it ineligible for emission.

In Fig. 5, we show initial simulation results on electron emission from rough and flat Sb photocathodes. The spectral response of the QE from grated rough surfaces is higher than from flat ones. Moreover, as expected, the QE is higher when the electron MFP is higher since electrons survive over a longer period of time before the first scattering event. This allows more electrons to reach the emission surface with sufficient energy to be emitted into the vacuum sub-region.

We also run similar simulations with GaAs as the emissive material. For GaAs, the behavior was reversed: the QE from flat GaAs surfaces was slightly higher than from the 3-ridge rough surfaces over a range of photon energies that span the electron affinity of GaAs used in the simulations.

SUMMARY

We implemented modeling capabilities to simulate electron emission from Sb photocathodes with controlled rough surfaces in the 3D VSim PIC code. The QE from rough Sb surfaces was higher than from flat ones. This behavior is reversed when using GaAs for the photocathode. However, the electron dynamics in GaAs is very different compared to Sb. In GaAs, scattering is dominated by low-energy phonon processes allowing electrons to survive for much longer time also leading to much higher QE values. We are currently in the process of extending our models for electron excitation in Sb (taking into account accurate representation of the DOS [8]), time-varying laser pulse absorption at oblique incidence, and surface-varying (due to interference) light intensity. These are additional capabilities needed to model momentatron experiments.

REFERENCES

- [1] D. H. Dowell *et al.*, *Nucl. Instr. Meth. Phys. Res. A*, vol. 622, p. 685, 2010.
- [2] J. Feng *et al.*, *Rev. Sc. Instr.*, vol. 86, p. 015103, 2015.
- [3] J. Feng *et al.*, *Appl. Phys. Lett.*, vol. 107, p. 134101, 2015.
- [4] B. Ziaja *et al.*, *J. Appl. Phys.*, vol. 99, p. 033514, 2006.
- [5] D. A. Dimitrov *et al.*, *J. Appl. Phys.*, vol. 108, p. 073712, 2010.
- [6] S. Karkare *et al.*, *J. Appl. Phys.*, vol. 113, p. 104904, 2013.
- [7] D. A. Dimitrov *et al.*, *J. Appl. Phys.*, vol. 117, p. 055708, 2015.
- [8] D. W. Bullett, *Solid State Commun.*, vol. 17, p. 965, 1975.